

## Chapter 6

# 3D-Molding of Microfluidic Devices

### 6.1 Introduction

Multilayer elastomeric device fabrication by replication molding requires a method for bonding together layers. In our development of solvent-resistant microfluidics, the goal with each promising new material or coating was to fabricate multilayer chips to evaluate crossed-channel valve performance and ultimately to implement functional elastomeric devices. However, determining a reliable adhesion process was often a significant obstacle (see Chapters 3, 4, and 5). Because methods can rarely be re-used in different material systems, development of bonding protocols was time consuming, slowing progress and limiting the number of materials that could be thoroughly investigated. Generic bonding methods such as gluing are generally not useful due to the presence of easily clogged microfeatures on the bonding surfaces and due to the incompatibility of glues with many solvents that might be flowed through channels. Surface chemistry modification and partial curing techniques are usually required.

To speed up our investigations, we developed a novel replication molding procedure based on sacrificial 3D wax molds, which eliminates the need for layer bonding entirely. A single mold contains a 3D pattern of fluid and control channels and a complete multilayer elastomeric device can be cast in a *single* step. We have demonstrated functional crossed-channel microvalves in elastomeric devices cast from these molds. While the resulting devices are of lower quality than those obtained by silicon wafers patterned with photoresist, this technique accelerates the ability to evaluate oper-

ational parameters such as modulus, porosity, and chemical compatibility of novel polymers within the context of functional microvalve networks. At the same time, the range of possible device materials is potentially broadened since one can use materials for which adhesion may be impossible or impractical, due to the presence of particularly stable surfaces or due to the lack of sufficient information such as is the case for materials with unknown (often proprietary) structures.

Despite the original motivation of eliminating the need for layer bonding, the general principle of 3D fabrication offers a number of other advantages. The most obvious is more topological flexibility. Instead of having the network of fluid channels confined to a single 2D layer as in two-layer PDMS chips, fluid channels can be routed vertically, enabling fluid channels to pass over one another. Another benefit is the reduced number of fabrication steps for complex fluidic components. 3D fabrication techniques also enable structures that cannot simply be fabricated by other means—those that are very tall, that have extremely high aspect ratios, or that have complex geometries and topologies. Expanding into the third dimension may also enable increases in chip densities.

This chapter begins with an introduction to a variety of existing methods for 3D microfluidic fabrication, followed by a description of our molding process. Next, details and results of our channel and integrated valve fabrication tests are presented. The chapter concludes with further discussion of some of the possible applications for 3D microfluidic fabrication.

## 6.2 Fabrication technologies for 3D microfluidics

Within the enormous literature of microfabrication, there are countless reports of fluidic networks constructed by almost every imaginable process. In this section, I provide an overview of these processes, deliberately limited to those methods having some intrinsic 3D capability. This includes the fabrication of channels having three-dimensional paths and networks having multiple layers of channels.

There are at least three general approaches for making 3D microfluidic devices: (i) layered fabrication (requiring bonding); (ii) direct 3D fabrication; and (iii) 3D molding. Whether fabricating device layers, whole devices, or molds, a wide range of tools are available, including stereolithogra-

phy, photolithography, solid-object printing, and mechanical or laser machining. The remainder of this section provides some introduction to the available techniques, including their capabilities and limitations.<sup>1</sup>

### 6.2.1 Layered fabrication

Thin layers containing vias and two-dimensional channel patterns can be stacked and bonded to form three-dimensional microfluidic networks of arbitrary topological complexity. Generally each layer is made by a relatively simple machining or molding process. The main drawback is the large number of time-consuming precision alignment and bonding steps needed to assemble the layers.

The two-layer PDMS devices developed in our lab are a familiar example of the layered fabrication approach. In fact, the process can be repeated to stack additional channel layers [272]; however, it has not been practical to fabricate vias between specific layers. Variations of the process have been demonstrated that exhibit more flexibility in this regard. For example, Jo *et al.* [137] reported the fabrication of complex structures including a 5-layer cascading channel and reservoir network and a three-dimensional passive serpentine micromixer. Their method involves the creation of two-dimensional PDMS membranes by curing prepolymer between a silicon wafer patterned with SU-8 photoresist clamped to a flat plastic sheet. After curing, the plastic sheet is removed and the membrane is peeled from the silicon wafer to be assembled into the 3D device. Each membrane has a thickness matching that of the resist (100  $\mu\text{m}$ ) and contains vias (and other shaped openings) where photoresist was present on the wafer. Alignment within about 15  $\mu\text{m}$  was facilitated by: (i) fabricating membrane layers of identical shape and size and aligning corners; and (ii) including common holes through each layer to promote self-alignment by surface tension when methanol is placed between oxygen plasma treated layers. Jeon *et al.* [134] reported a slight variation of this method, perhaps capable of thinner layers because a special pressure-sensitive adhesive tape is applied to the membrane for ease of handling during plasma bonding to the previous layer in the

---

<sup>1</sup>Numerous other physical processes have been used to generate microscale patterns, including fluidic self-assembly, colloidal sedimentation, polymer phase-separation, and templated growth. However, most currently permit only simple geometric patterns or coarse control over bulk properties and are not suitable for creating arbitrary microfluidic structures: they have therefore been omitted from the discussion.

device. Diaphragm and flap check valves were demonstrated, though more complex networks are also possible. An alignment accuracy of about  $10\ \mu\text{m}$  was achieved using an  $x$ - $y$ - $z$  translation jig. A superior alignment jig permitting  $1$ – $2\ \mu\text{m}$  accuracy has been reported by Kim *et al.* [150].

Anderson *et al.* [5] reported another variation in which each single membrane contains three layers of features—channels in the upper and lower surfaces, and vias completely through the membrane. Membranes were fabricated by curing PDMS prepolymer between two facing molds, each having features of two different heights. The taller parts of the molds contact each other if sufficient force is applied and thus create vias in the membrane, while the short parts create channels. Proper registration is achieved by the use of mechanical alignment features. Mold release was facilitated by making one mold out of PDMS that can be easily peeled away, allowing one surface of the membrane to be bonded to another membrane before removal from the second mold. An  $8\times 8$  basketweave pattern of channels  $70\ \mu\text{m}$  deep by  $100\ \mu\text{m}$  wide and a helical channel surrounding a straight channel were fabricated. Note that the basketweave structure has features in 3 layers and is implemented entirely in a single membrane (though its floor and ceiling must be sealed); the helix has 5 layers of features and requires two membranes. This method reduces assembly steps at the expense of more complex molds. While not demonstrated, it should be possible to create 3D structures containing pressure-actuated crossed-channel valves in many layers. While technically not a lamination approach, another interesting variation was reported by Wu *et al.* [295]. In this method, a patterned membrane was sealed to another flat PDMS membrane, and individual channels were “cut out” as thin tubes that could be manually tied into interesting structures such as knots, helices, and weaves. In some cases the channels were held in place by threading through holes in a specially patterned PDMS membrane. The entire structure was then filled with PDMS to yield a final monolithic device. An additional technique was described in this paper: a PDMS layer containing embedded channels open to the side is slipped onto photoresist posts on a silicon mold pattern. When PDMS is poured over this assembly, the result is a monolithic device containing a 3D channel network composed of the channels in the original device connected to the channels defined by the silicon mold pattern in a perpendicular plane.

These procedures are in principle compatible with any material that can be molded and bonded, and have also been used in conjunction with melt processing of the biodegradable plastic, poly(DL-lactic-co-glycolide) 85:15 (PLGA 85:15) [151]. Polymer pellets were melted between two molds to create membranes with channels 2  $\mu\text{m}$  in width. Pressure and heat were applied to membrane stacks for extended durations to induce bonding by polymer-chain interdiffusion. Also reported in this work is an interesting technique for extruding integrated annular stubs onto which external microtubing can be connected.

Lamination has also been widely used in metal and ceramic microreactors that must withstand harsh conditions such as high temperatures, high pressures, organic solvents, plasmas, or microexplosions. Layering is the only way to produce high aspect ratio channels in these materials due to the difficulty of machining deep microchannels from the surface. The large interfacial area provided by the high aspect ratio is useful in applications requiring rapid heat transfer to or from the walls, or requiring rapid mass transfer across a membrane. High aspect ratio channels are also effective in reducing dispersion in analyses where the fluid must follow a serpentine path [55]. Among other devices, Martin *et al.* [181] of PNNL fabricated a laminated solvent-exchange device from a diffusion-bonded stack of several hundred layers of 100  $\mu\text{m}$  thick 304 stainless steel shimstock (foil). Each foil layer is patterned by photochemical etching or a stamping process. The device contains two layer patterns stacked alternately: (i) perforated layers to act as porous membranes; and (ii) layers containing 1 $\times$ 8 cm rectangular holes to act as very wide, shallow channels (channel depth is equal to the foil thickness). Lamination with ceramics was also reported, in which devices were made from stacks of laser patterned 125–250  $\mu\text{m}$  thick green (unfired) ceramic tape. The assembled stack is fired to eliminate the binder, leaving the all-ceramic device.

Glass is also somewhat difficult to machine, but has the desirable properties of stability, inertness, and transparency. Kikutani *et al.* [148] report the fabrication of layered 3D glass microfluidic chips for diffusively-mixed continuous flow combinatorial synthesis. The chip contained 4 inlet ports for two pairs of reagents and 4 outlet ports for all possible combinations of reactions between the two pairs of inputs. A three-dimensional chip was needed in order to accommodate several fluid channel

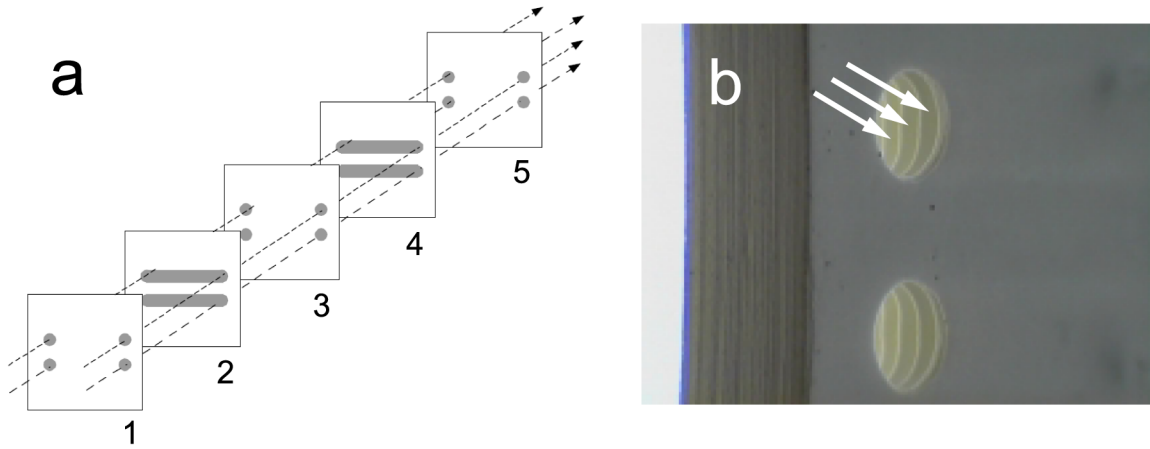


Figure 6.1: **3D laminated ceramic microfluidic device.** (a) Assembly diagram of a simple laminated device showing five layers. The slots cut from layers 2 and 4 will become microchannels, while the holes cut in layers 1, 3, and 5 will become headers (vias) to connect all the channels in parallel. The pattern of vias determines the flow pattern through the device, such as parallel flow (in this case) or serpentine flow. (b) Photograph of a ceramic device, with several thin channels visible through the header hole indicated by arrows. (Adapted from [182]. Copyright the American Institute of Chemical Engineers, 2000.)

crossings. It consists of three thermally bonded Pyrex glass plates—an upper and a lower layer containing etched channels ( $240\ \mu\text{m}$  wide by  $60\ \mu\text{m}$  deep) and a middle layer containing vias. A 10-layer assembly was reported in [270].

### 6.2.2 Direct 3D fabrication

When alignment and bonding are undesirable, methods are available for direct monolithic 3D device fabrication, including stereolithography, micromachining, and solid-object printing.

A variety of other techniques, such as CNC (computer numeric control) machining [305] and micromilling [221], wire EDM (electrical discharge machining), ultrasonic machining, acoustically-encoded groove cutting [73], spark-assisted etching, and laser cutting and drilling have been used to cut microchannel structures in a wide variety of materials, including glass, ceramic [181], metals, and hard plastics. Automated machines are capable of complex 3D patterning with resolutions down to  $10\text{--}20\ \mu\text{m}$  by cutting from multiple axes; however, because material can only be removed from the surface, complex 3D fluidic network geometries are not possible. Typically, fabricated devices are 2D networks of channels with channel depth variations, sometimes used in laminated devices.

In the remainder of this section, fabrication by stereolithography and photolithography are discussed in more detail. Solid-object printing will be discussed in Section 6.2.3 since to our knowledge, this technique has never been used to fabricate devices directly.

### 6.2.2.1 Stereolithography

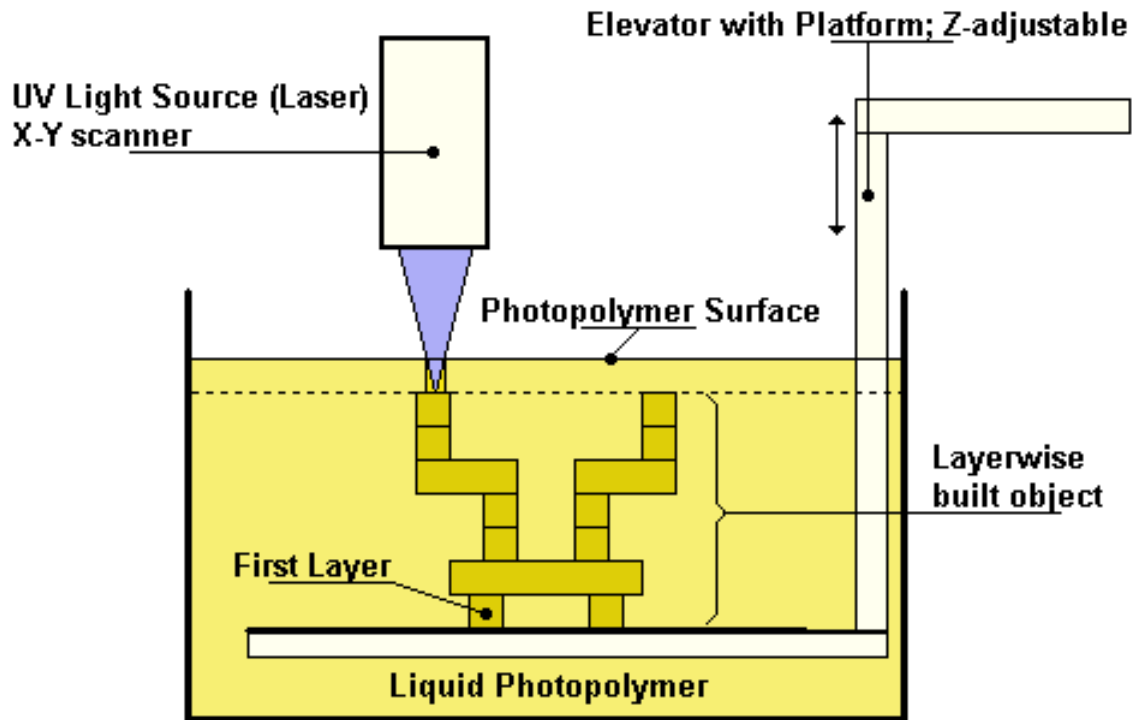


Figure 6.2: **Schematic of stereolithography process.** A monolithic 3D object is built up one thin “slice” at a time from a liquid photosensitive resin. A UV laser scans a 2D pattern representing one slice of the object in a thin layer of fresh resin at the surface, solidifying the exposed regions. To build subsequent layers, the sample is lowered further into the resin, and a new thin resin layer covers the top surface. This process is repeated until the object is complete, whereupon a developing procedure removes the unpolymerized resin. *Two-photon* stereolithography is similar; however, it is the position of the laser focus that moves vertically rather than the platform. Resolution is improved because problematic surface tension effects are eliminated and because non-linearities result in a smaller polymerized voxel size. (Reproduced from <http://www.proform.ch/en/t.sl.htm> with permission. Copyright PROFORM AG, 2005.)

Stereolithography is generally an additive process in which selected regions within a vat of photosensitive liquid resin are solidified via polymerization or crosslinking upon exposure by a focussed UV laser beam (see Figure 6.2). Rapid prototyping stereolithography machines are commercially

available, albeit very expensive, and can fabricate complex objects from 3D CAD (computer aided design) drawings entirely automatically. In one approach, the object is constructed by sequentially solidifying additional “slices” of the object at the surface. Depth resolution is limited by the layer thickness. In the related technique known as *selected laser sintering*, the object is built up from a thermoplastic powder, sometimes combined with ceramics or metals. In a variation of these methods, the position of the laser focus is controlled in *three* dimensions, allowing improved fidelity because polymerization occurs deep within the resin where there are no problematic surface tension effects. Non-linear effects are needed to ensure a small polymerization volume near the focus without polymerization of all material through which the beam passes. In the two-photon technique a photoinitiator is used having sensitivity only to twice the laser photon energy. Only at the focus of a pulsed femtosecond laser is the intensity sufficient for two-photon absorption to occur. With non-linear material response, voxel sizes of 100 nm (below the diffraction limit) have been reported under optimized exposure and development conditions.<sup>2</sup> Another non-linear process is based on a temperature sensitive resin that polymerizes only if a temperature threshold is reached. Yamakawa *et al.* [298] report a very inexpensive implementation of this technique, wherein a CD-player pickup laser is employed for polymerization. An extensive review and history of photopolymerization chemistry and technology can be found in [261].

Several investigators have fabricated microfluidic devices using stereolithography. Kang *et al.* [141] fabricated several design variations of a 3D blood-typing system and employed a computer solidification model and the concept of “unit” components to improve fabrication reliability. Ikuta *et al.* [118] fabricated a microfluidic device integrated with a silicon sensor and demonstrated an electrostatically actuated flap valve constructed from a conductive polymer. Employing photogenerated acids, Zhou *et al.* [308, 304] performed *subtractive* two-photon stereolithography by *photodepolymerization*. A simple device containing twelve 50  $\mu\text{m}$ -long  $4\times 4$   $\mu\text{m}$  square channels buried 10  $\mu\text{m}$  beneath the surface was fabricated. The main limitation is the risk of overdevelopment if the time to remove material from long narrow channels is too great. However, the subtractive method significantly

---

<sup>2</sup>Impressive demonstrations of complex objects produced by two-photon stereolithography include a 10  $\mu\text{m}$  sculpture of a bull [143] and a chain with 50  $\mu\text{m}$  links [154].

speeds construction as one needs only excavate the channel and reservoir regions within a large solid body rather than building up walls around every microfluidic channel. Sugioka *et al.* [260] describe a different subtractive two-photon method based on photo-etchable glass. Upon exposure to UV radiation and subsequent heat treatment, exposed areas form a crystalline phase within the amorphous glass that has a much faster etch rate in dilute HF. Several microfluidic structures were demonstrated, including a Y-shaped microchannel (20  $\mu\text{m}$  wide by 70  $\mu\text{m}$  deep) located 300  $\mu\text{m}$  below the sample surface, and a Y-shaped channel in a vertical configuration, extending 2 mm between front and back surfaces of the glass. The authors also fabricated a vertical structure containing a tiny movable glass plate that could be switched between two positions using compressed air and thus could serve as a microvalve. Despite some drawbacks (large valve size, two dedicated control inputs required, and possibly incomplete sealing), the valves could enable the fabrication of complex fluid-handling networks in a variety of hard, inert materials. However, it is not clear whether the etch rate difference (about 45 $\times$ ) is sufficient to reliably produce very long narrow channels. Note that this example illustrates an important capability of subtractive direct-writing methods—the ability to form freely moving components.

Stereolithography is an expensive method for fabricating 3D microfluidic devices but has very high resolution, has complete three-dimensional freedom, and can simultaneously accommodate microscopic and macroscopic features. It is compatible with any material having appropriate photo- or thermosensitivity. The two-photon volume polymerization approach is only compatible with transparent resins. To our knowledge, elastomeric materials have not yet been patterned by stereolithography. However, it is possible that laser ablation could pattern cavities and microchannels in PDMS and other transparent materials in an analogous manner to subtractive two-photon stereolithography. Maltezos [177] observed that a focussed laser beam could ablate PDMS to generate cavities in the interior of a sample. Little is currently known about the fabrication characteristics of this approach. Stereolithography could also be used to print 3D molds.

While somewhat different than stereolithography, Hutchison *et al.* [116] report the fabrication of 3D devices by a photopolymerization technique called contact liquid photolithographic photopoly-

merization (CLiPP). A thin layer of liquid monomer is poured into a chamber, polymerized in desired regions by exposure through a photomask, and finally developed to remove the uncured monomer. Molten wax is then poured into channels and solidified, serving as a sacrificial material and providing a flat surface on which to build the next layer. A new layer of monomer is poured on the surface, and the process is repeated until the object is complete, whereupon the wax is removed. Compared with stereolithography, this technique offers considerable speed advantage due to the parallel exposure and also offers the opportunity to incorporate different materials in different layers. Surface modification is straightforward and can provide particular functionalities and covalent bonding between materials in different layers. The authors demonstrated the fabrication of a 3D microfluidic device containing multiple layers of channels, a freely rotating flow meter, and a device containing an integrated photopolymerized heating electrode. Elastomeric materials have been used with this method, and though rounded channels were not reported initially, such channels can be created by polymerizing the first layer on an appropriate mold (to make push-down microvalves) [115].

#### **6.2.2.2 Micromachining and photolithography**

Sophisticated microfluidic devices have been fabricated with silicon, glass, metal, and PDMS by a variety of micromachining processes common in the field of MEMS, including photolithographic patterning of resists, bulk micromachining, surface micromachining, and LIGA (Lithographie Galvanoformung Abformung). These tools can be used either to make molds or to make devices directly—both will be discussed here for the sake of continuity. Though most micromachining techniques are inherently 2D processes, 3D devices can be fabricated by combining them in clever ways. As a simple example, Liu *et al.* [171] fabricated a 3D serpentine mixer in silicon by etching from both the top and bottom. Regions where only one side is etched form channels; regions where both sides are etched become vias completely through the wafer, joining the two channel layers. In principle additional layers can be deposited and patterned to build up complex 3D networks; however, due to the large number of processing steps, this tends not to be a very practical approach.

Aside from micromachining techniques, methods have been reported to fabricate 3D structures out of photoresist by carefully crafted exposures and often a single developing step. Such processing is in many ways a special case of stereolithography, but having different exposure mechanisms. To achieve some limited 3D control of the exposure, techniques such as multiple exposures, tilted exposures, controlled depth exposures, and exposure by 3D interference patterns have been used. Photolithography can be substantially faster than stereolithography, if (parallel) flood exposures are used. Mold patterns with multiple height features, as well as fully three-dimensional devices and molds, have been demonstrated.

Multiple exposures with different penetration depths were used by Kim *et al.* [149] to create structures with three distinct layers of features in 80  $\mu\text{m}$  thick positive photoresist. Shallow front and back exposures defined the pattern in the top and bottom 20  $\mu\text{m}$  layers, while a deep front exposure through the entire resist layer delineated boundaries between structures. This technique can be used for direct fabrication of microchannel structures or can be used to make molds. Fluidic networks with crossing channels, or channels with surface textures such as grooves, pillars, or pits are possible.

Romanato *et al.* [231] created microfluidic channels in PMMA photoresist via tilted X-ray exposures. Exposing twice through a mask at different tilt angles (differing by a  $180^\circ$  azimuthal rotation of the sample) generated two leaning walls of resist that intersected to form a long hollow 11  $\mu\text{m}$  deep microchannel parallel to the surface with a downward-pointing triangular cross-section. In addition, they demonstrated a “fence” structure (standing vertically on the surface) that could perhaps be used in size-selective filtering.

Kudryashov *et al.* [153] employed UV exposure through greyscale masks combined with e-beam writing to fabricate interesting structures in SU-8 photoresist. E-beam illumination penetrates only a few microns into the upper surface, while UV illumination generates structures in the bulk of the resist. The height of UV-exposed structures depends on dose, permitting molds or devices with carefully designed channel profiles (e.g., rounded profiles for closable fluid channels), or complex multi-depth features. An interesting demonstration was the construction of a series of 15  $\mu\text{m}$  tall

posts supporting a thin (several microns) flexible “net” structure with a square mesh. The authors suggest that the mesh size can be varied between 2–100  $\mu\text{m}$  and that the nets might be useful as traps for soft objects such as biological cells. One could also imagine using this technique to fabricate molds for 3D fluidic networks with crossed channels.

The use of multiple beam exposure, or exposing through phase masks, generates an interference pattern throughout the volume of the resist. Carefully designed interference patterns can selectively expose regions *inside* the resist layer, unlike conventional exposure that progresses through the material from the surface. Generally it is only possible to generate 3D structures that are mostly periodic with feature size on the scale of the illumination wavelength; therefore these methods are probably better suited to the fabrication of components such as integrated filters, gratings, and photonic crystals rather than complex 3D channel networks. Jeon *et al.* [135] report the fabrication of a Y-shaped channel in SU-8 having an integrated nanofilter using the combination of a conventional amplitude mask for the channel and a phase mask for the filter.

Control over exposure at different depths within the resist can also be achieved by using multiple resist layers. Exposure can occur in between deposition of subsequent layers, or resists can be selected that have orthogonal processing conditions and exposure radiation sensitivities. Romanato *et al.* [231] created molds from three layers of resist to create a network of microtanks connected by channels. A thin layer of SAL photoresist on a thick PMMA layer was exposed via e-beam lithography and developed, yielding a pattern of SAL microwires (0.2–1  $\mu\text{m}$  wide) on top of the unaffected PMMA. A second PMMA layer was deposited and then the entire structure exposed via X-ray lithography, leaving a pattern of double-height PMMA posts connected by SAL microwires at mid-level. The microfluidic device was then created by electroforming with gold and then removing the resist. Yoon *et al.* [302] used a sequential process to build up complex microfluidic networks in nickel. Each photoresist layer was patterned via controlled depth exposures to build structures with two heights and was then electroplated with nickel up to the same height, providing a level surface on which to spin the next resist layer. Once complete, the resist was removed, revealing a complex network of channels (from short resist features) and vias (from tall resist features).

The above photoresist patterning methods and most micromachining techniques are performed with hard materials, in which mechanical valves have only been demonstrated by very elaborate fabrication methods [300, 285]. Fully elastomeric devices based on integrated crossed-channel valves could be fabricated by molding from microfabricated molds.

### 6.2.3 3D molding

Molding is a process whereby the desired three-dimensional pattern of empty spaces (microchannels, microreactors, and other fluidic components) is defined. The mold comprises the “inverse” of the desired structure. Thus, for example, a microfluidic channel would be represented in the mold by a long thin *beam*. The final microfluidic device is fabricated from the mold by embossing (if there are no suspended features), casting, or injection molding. If the mold contains suspended features, it must be sacrificed in order for the device to be removed.

Molds must have sufficient structural integrity to maintain their shape prior to casting. In microfluidic designs that are sensitive to the vertical distance between channels (e.g., those having crossed-channel valves), long thin beams that are prone to sagging must either be avoided or be supported by pillars near critical gaps. Since pillars will leave voids in the final microfluidic device, they should be positioned so as not to interfere with fluid flow or other aspects of device operation. When pillars are needed, usually only a few layers of microchannels are practical. In fact, we found it simplest to route most channels along the mold substrate in two dimensions, only utilizing the third dimension when channel crossings, valves, or inherently 3D fluidic components were needed. Due to this constraint, molding does not generally offer as much design flexibility as direct fabrication methods such as stereolithography.

The primary advantage of molding is the elimination of alignment and bonding steps that are needed in layered fabrication. 3D molding also has an advantage with respect to stereolithography in that a much wider range of potential device materials can be used—there is no need for temperature or photosensitivity nor transparency. With molding, there are only a few restrictions on the device material: it must be chemically compatible with the mold, and it must have sufficiently low viscosity

to fill the smallest cavities in the mold. Of course, the curing conditions of the device material must be tolerable by the mold material, and the final device must be inert to the mold removal conditions in the case of sacrificial molding.

Molds for microfluidic devices are most frequently fabricated by micromachining as discussed in the previous section, but have also been fabricated by solid-object printing and several other interesting methods. As one example of these other methods, Dharmatilleke *et al.* [63] cast PDMS on sacrificial molds made by manually drawing molten wax into thin filaments 100–200  $\mu\text{m}$  in diameter. The wax was dissolved to leave circular profile microchannels. Branched networks were created by “soldering” filaments together, and complex 3D channel shapes such as helices were also demonstrated. Another example is the use of micromilling with toolbits of 20–25  $\mu\text{m}$  diameter to fabricate (non-sacrificial) brass molds for a 3D serpentine mixer [12].

Solid-object printing is perhaps the most attractive mold-making option. With the availability of commercial ink-jet and thermoplastic extrusion machines, an entire 3D mold structure can be fabricated directly from a CAD file in a single unattended run. These printers generally cost much less than stereolithography machines to own and operate and have the additional advantage that multiple materials can be incorporated into the 3D object. For example, use of an easily removable sacrificial material allows the construction of elaborate suspended or even freely moving structures from another material. When the final mold itself is to be sacrificial, the mold material is typically a polymer, but ink-jet printing is also capable of printing other materials such as fused powders and metals [34]. Compared with micromachining and photolithography, solid-object printing does not require a clean room or specialized equipment such as mask aligners, exposure systems, and spin coaters, nor are toxic chemicals such as photoresists and developers required during processing. Printers can accommodate structures with a wide range of sizes, including very tall features that are not possible with photolithography due to thickness limitations of available resists (0.5–1.0 mm). Drawbacks of solid-object printing include high surface roughness and relatively poor resolution.

Cooper *et al.* previously demonstrated the use of a ThermoJet solid-object printer to fabricate molds for PDMS microfluidic devices [187]. This particular printer cannot fabricate suspended struc-

tures, so cast devices were simply peeled from the mold and sealed to a substrate. The minimum feature size (in all dimensions) was about  $250\ \mu\text{m}$ . High surface roughness ( $8\ \mu\text{m}$ ) interfered with sealing of the PDMS device to substrates, particularly glass. The authors circumvented this problem by first fabricating the inverse of the desired mold, annealing its top surface against a flat transparency film, and then casting a PDMS replica that would serve as the actual mold. This process resulted in a flat bottom surface for bonding but did not improve roughness of channel walls. Several devices were fabricated, one consisting of 2 channels in the  $x - y$  plane plus a vertical channel of 5 mm length above their intersection designed to hold an optical fiber for imaging. Another device was a chaotic advective mixer consisting of a microchannel with a staggered series of groove patterns in the floor, previously fabricated by double photoresist [258] or laser photoablation techniques. An immunoassay device was implemented with ports compatible with a 12-channel pipettor, demonstrating simultaneous fabrication at micro and macro scales. Finally, using the lamination strategy described in Section 6.2.1, two molds were printed with alignment features and used to create a 3D basketweave pattern [5]. The poor resolution, especially in the vertical direction ( $250\ \mu\text{m}$ ), prevents the fabrication of crossed-channel microvalves.

In the next section, I describe our own work to print molds for microfluidics using a similar approach. Significant differences in our work include: (i) much improved resolution, with features as small as  $13\ \mu\text{m}$  in  $z$  and about  $200\text{--}250\ \mu\text{m}$  in both  $x$  and  $y$ ; (ii) the ability to print molds directly on a flat substrate, obviating the need for an inverse mold and annealing step; (iii) the ability to print two materials—one acting as a structural mold material and the other acting as a sacrificial material—thus enabling the construction of buried and crossed channels without the need for multiple molds or layer bonding; and (iv) the demonstration of functional valves, including a crossed-channel microvalve—a first step towards sophisticated 3D fluid handling. The channel network of an entire typical two-layer elastomeric device can be represented on a *single* sacrificial mold and can be embodied in a microfluidic device in a single casting step. This enables the rapid evaluation of the performance of new materials in active microvalve devices without the need to first develop a layer bonding procedure.

## 6.3 Device fabrication from 3D wax molds

### 6.3.1 Mold fabrication

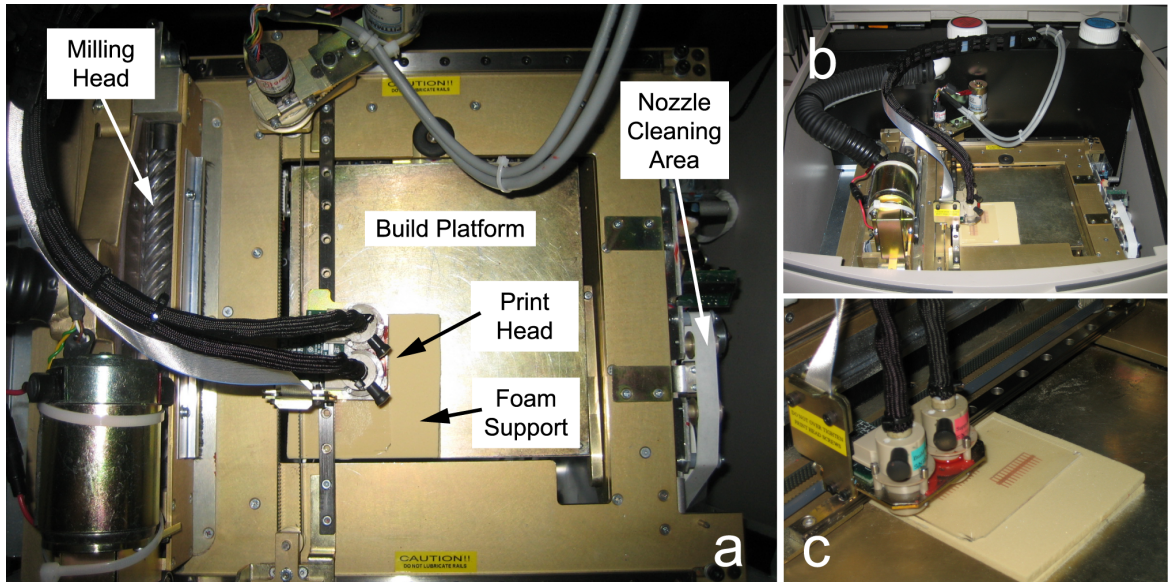


Figure 6.3: **Solidscape T66 3D ink-jet printer.** (a) Top view of the Solidscape T66 with the cover open. The large central square is the vertically moving build platform. A mold is being printed on a 2×3 inch glass slide (barely visible) glued to a square piece of foam support that is affixed to the lower left corner of the build platform. After printing the layer the print head will move to the far right for ink-jet nozzle cleaning. After allowing time for wax cooling, the milling head at the left begins spinning and passes over the mold left to right and back. The entire build platform then moves downwards to make room for the next layer. (b) Wide angle view of the printer showing a few elements not visible from the top: the vacuum hose connected to the milling head and the reservoirs for the build wax (blue) and support wax (red) at the rear of the machine. (c) Close-up view of the two ink-jet nozzles on the print head during printing of a mold.

Three-dimensional sacrificial wax molds were printed with a Solidscape T66 high resolution solid-object printer (see Figure 6.3). Mold patterns representing the inverse of the desired channel network were designed in SolidWorks (a 3D CAD program), exported in STL file format, and processed by ModelWorks for translation into the printer-readable t6 file format. ModelWorks divides the design into layers of the selected thickness (13–76  $\mu\text{m}$ ) and automatically adds support material to each layer as needed (e.g., for suspended features). Molds are printed one layer at a time on a 6-inch-square “build platform” within the machine by a print head moving in the  $x$ - $y$  plane. Ink-jet nozzles deposit tiny droplets of molten wax approximately 75  $\mu\text{m}$  in size [120]. Since droplets are deposited approximately every 5  $\mu\text{m}$ , they overlap and provide reasonably straight edges on features. To

ensure a uniform thickness of new wax material and a flat surface on which the next layer is built, a milling head cuts across the entire model after each layer is printed and cooled. The platform is then lowered by the layer thickness to make room for the next layer, and the cycle is repeated until the object is complete.

At the start of a print run, a jet cleaning and calibration procedure is performed to ensure that droplet volumes are consistent and that no air bubbles are present in the nozzles. The temperature controlled chamber further improves consistency by ensuring repeatable impact behaviour of droplets. Next, a piece of rigid foam (provided by Solidscape) or balsa wood is affixed to the build platform. (Initially we had used a softer foam provided by Solidscape, but its ability to deform resulted in poor printing accuracy.) The foam support is milled down in progressively smaller increments until level and flat. The milling head is then carefully cleaned to prevent dust from falling on the pattern during printing. In normal operation, solid objects are printed directly on the foam surface. However, the foam is not suitable as a mold substrate for casting microfluidic devices from liquid prepolymers due to its roughness and porosity. Instead, we affixed a 2×3 inch glass slide or untreated silicon wafer on top of the foam (using a glue stick). To prevent the milling head from hitting this new substrate, the build platform was manually moved down by a distance equal to the added thickness. This distance was determined by the difference of two Vernier caliper measurements—one of the platform and foam thickness immediately after milling the foam, the other of the platform, foam, and new substrate thickness after gluing. Accuracy is critical: if underestimated, the milling head can contact the substrate, resulting in complete removal of the first few wax layers or in damage to the substrate; if overestimated, the first layer may be very thick and irregular and the increased jet-substrate distance can result in poor printing quality. Once the build platform is properly lowered, printing proceeds normally on this new substrate. We found pattern quality to be somewhat better on glass than silicon, perhaps due to the better adhesion of wax to the uncleaned glass surface. The use of a glass or silicon mold substrate leads to a smooth bottom surface of the microfluidic device cast from the mold, suitable for bonding the device to a flat, glass bottom plate. Prior to the development of this method, we incorporated a rectangular slab in our design files, resulting in the

mold features being built on wax slab. However, we experienced device bonding problems due to the relatively high surface roughness of the wax—approximately 1–2  $\mu\text{m}$  (RMS), according to measurements with an Alpha-step 500 profilometer (KLA-Tencor), in agreement with the specifications provided by Solidscape [119]. Typical surface height variation is  $\pm 2.5 \mu\text{m}$  with excursions up to  $\pm 7\text{--}8 \mu\text{m}$ . Use of the flat glass or silicon substrate solved this problem, but it should be noted that other surfaces of mold features (e.g., channels) remain rough.

In constructing each layer of the 3D pattern, two types of wax are printed by dedicated ink-jet nozzles—one is “build” wax from which the final 3D mold is made; the other is “support” wax and serves the temporary functions during printing of providing a solid surface on which suspended mold features are built, and forming a wall around all features to provide lateral support during milling and to protect against contamination by dust particles. The ModelWorks output file specifies the movement path of the print head and the droplet firing positions. Paths are specified in a vector format, with outlines printed first and subsequently filled, to ensure high fidelity of edge positions and shapes, even on rounded features. Build wax is printed first, followed by support wax. To speed up printing and later support wax removal, the regions of support wax are printed as a widely spaced grid. This caused us some problems in early design iterations, as the grid size was larger than the area of our crossed-channel microvalves, occasionally resulting in the absence of support wax in the critical gap between the two channels on the mold. During printing, the channel beams were fused by build wax, resulting in the channels being directly connected when cast into a microfluidic device. This problem was solved with a modified configuration file provided by Solidscape that has reduced grid spacing. Note that because ModelWorks adds a fixed number of grid squares surrounding all features, the thickness of the protective support wax wall surrounding each feature was substantially reduced. Typical print time for a single layer is about 1–2 min including printing and cooling times.

Resolution of the mold in the  $z$ -direction is determined by the selected layer thickness, typically 12.7  $\mu\text{m}$  in our molds. Designed distances in this direction were accurately reproduced by the printer due to milling between layers. However, the presence of wax dust from milling that was not completely removed by the vacuum and brush system connected to the milling head caused some

problems. Dust particles that managed to get locked into the support material in the gap of a crossed-channel valve led to an open fissure between fluid and control channels in the microfluidic device cast from the mold. For this reason, vertical separations were designed to be at least several layers thick. According to specifications [119], the minimum feature size in the lateral directions ( $x$ - $y$  plane) is about  $250\ \mu\text{m}$ . Based on test patterns we created (see Section 6.4.1), we found a minimum feature size of about  $200$ – $250\ \mu\text{m}$ , with some variation depending on the state of the ink-jet nozzles—over time, the nozzles seem to print less accurately. We also found that features had to be separated laterally by at least  $65\ \mu\text{m}$  in the design to reliably be separated in the printed part. We had difficulty building very tall structures such as posts for inlet ports—these features were often distorted or toppled during milling steps, even when surrounded by substantial amounts of support wax.

Once the mold has been printed, it is removed from the foam block and immersed in a hydrocarbon solvent (BioAct VSO) to dissolve the support wax, which is no longer needed. The solvent is heated to  $60$ – $65^\circ\text{C}$  and gently stirred to accelerate support wax removal. Progress is visible due to the contrasting colours of the support wax (orange/red) and build wax (blue). Generally the final few minutes of this “dewax” process are performed in fresh solvent to minimize residue remaining after solvent evaporation. The mold is dried overnight at  $60$ – $65\ ^\circ\text{C}$  with the mold substrate tilted at an angle to encourage solvent to flow away from the pattern. If left flat, we have observed significant residue near mold features after drying. Incomplete support wax removal can lead to the appearance of a cloudy film over the substrate or to the appearance of sharp crystal shards on feature surfaces after drying, both interfering with the sealing of cast devices to flat substrates. It is critical that the VSO solvent be eliminated as thoroughly as possible as it interferes with the proper curing of PDMS and encourages bonding of PDMS to the glass or silicon substrate. Many of our early silicon wafers had small pieces of PDMS stuck after mold melting (described in the next section), which had been torn from the device as it was removed from the wafer. The problematic regions correlated well with regions where solvent would be expected to evaporate most slowly—tight corners. This and other problems encountered during development of the fabrication process are depicted in Figure 6.5.

### 6.3.2 Device fabrication

Microfluidic devices were fabricated by casting liquid prepolymer on a 3D wax mold, melting the mold, and then sealing the cured elastomer to a substrate such as glass, as summarized in Figure 6.4.

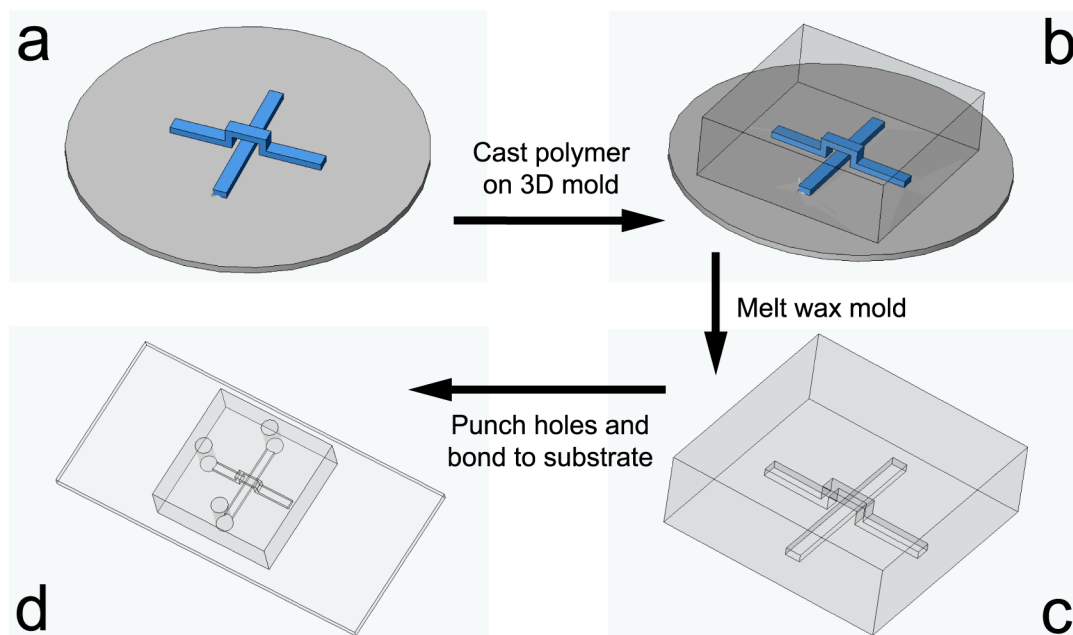


Figure 6.4: **Fabrication of microfluidic devices from 3D wax molds.** (a) After printing a 3D wax mold, support wax is removed by immersion in VSO solvent, after which the solvent is evaporated by heating. (b) Prepolymer is poured on the mold, degassed, and cured. (c) Once solidified, the polymeric device is released by melting the sacrificial mold and cleaning with solvents. (d) Holes are punched and the device is bonded to a substrate. No layer-layer bonding is required as the entire network of microchannels is replicated in a single casting step.

Prepolymer is first poured over the 3D mold and degassed until no further bubbles are observed to emerge from the smallest confined spaces (valve membrane regions) in the mold. To conserve material and to prevent leaking beneath the wafer that would complicate mold removal, a rectangular PDMS gasket is sealed to the mold substrate surrounding the pattern and filled with the prepolymer. The polymer is then cured by its normal processing conditions, modified if necessary to avoid destroying the mold. PDMS and Sifel were heat cured by baking at 60–65°C, a temperature selected to avoid melting the wax mold prior to polymer solidification. PFPE was cured in an ELC-500 UV curing chamber (Electro-Lite Corporation). Exposure for 1 min solidified the elastomer, and then the mold and PFPE were exposed for an additional 40 min with the orientation changed every 5 min

(normal cure time is 10 min). A wide variety of orientations were necessary to ensure UV exposure of all PFPE regions—the opaque blue wax structures prevent UV radiation from reaching the liquid between intersecting beams (valve membranes) if only top illumination is used.

Once cured, the device is removed by melting the wax mold. Above about 110–120°C, the wax rapidly melts to a low viscosity liquid and can freely flow out of the channels. With the wax in the liquid state, the whole device can be peeled from the substrate without risk of breaking entrapped polymer pieces. We did not have any difficulty removing PDMS or PFPE from the untreated glass slide or silicon wafer used as the mold substrate. The wax remaining in the channels can be further drained by continued baking in appropriate orientations and by subsequent immersion of the device in an organic solvent such as acetone or methanol. After drying the solvent by heating, holes are punched in the cleaned device to access both the fluid and actuation channels, and the device is bonded to a substrate to seal the “floor” of any channels or support pillars that were printed directly on the mold substrate. For example, a PDMS device can be covalently bonded to a cleaned glass slide by oxygen-plasma treatment (see Appendix A.2.4). Since both fluid and control channels may be in contact with the substrate, it is necessary that the bond strength be sufficient to withstand all pressures involved during device operation.

## 6.4 Results

My original goal was to produce devices from solvent resistant elastomers such as PFPE, FNB, and Sifel for further material evaluation and ultimately to perform chemical synthesis. However, due to the very short supply of solvent-resistant materials from our collaborators, PDMS was used as a surrogate during development and optimization of the 3D molding procedure. We first demonstrated the compatibility of the other materials with all aspects of the basic process<sup>3</sup> and then put them to better use investigating other methods of device fabrication in parallel.

---

<sup>3</sup>Had we found incompatibilities, we would have tried printing a negative relief version of the desired mold and casting an intermediate sacrificial material to serve as the mold for the microfluidic device. Presumably, one could also tap into the vast range of materials that have been printed with ink-jet technology [34] to find an alternative mold material.

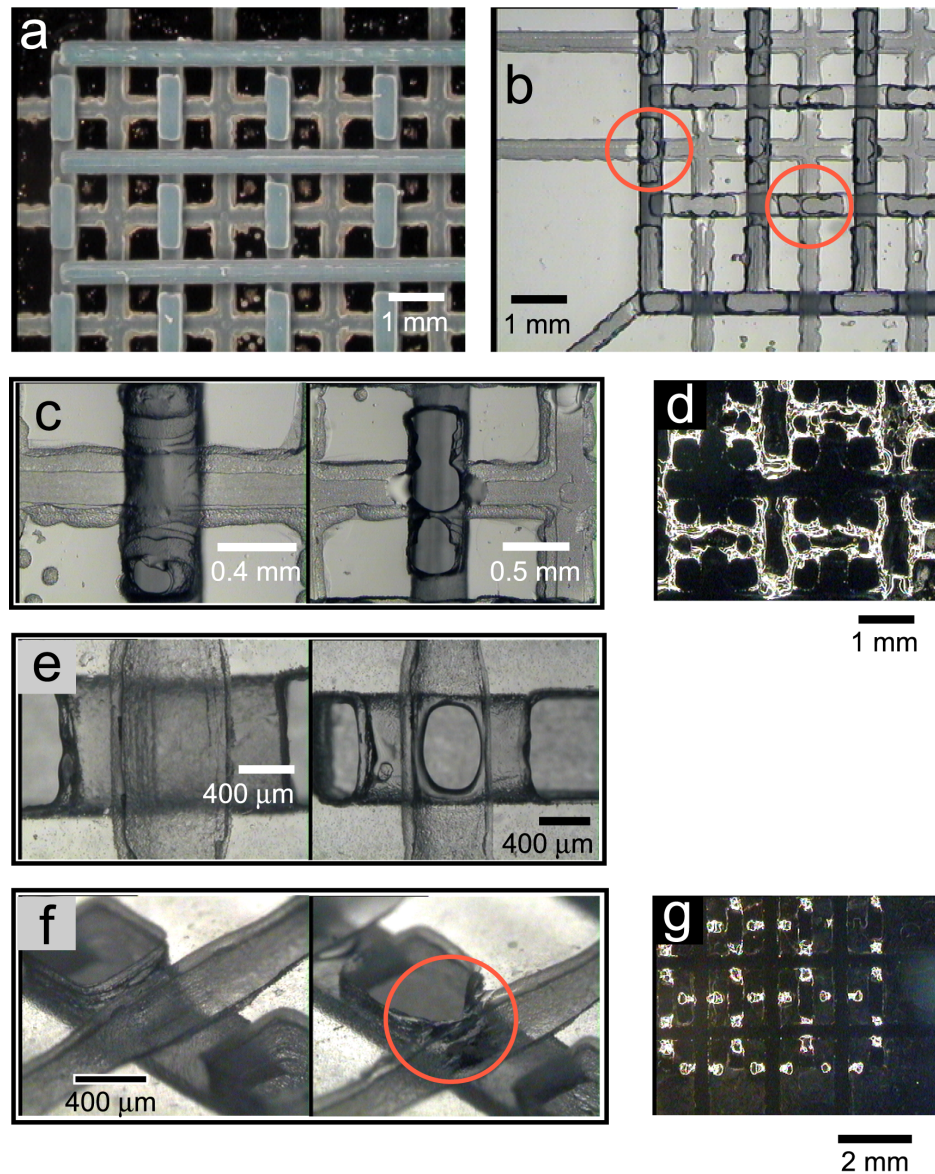


Figure 6.5: **Fabrication defects during protocol development.** (a) A micrograph of a mold after support wax removal illustrates the large amount of debris (dust and stray droplets) and the highly irregular edges of channel features that can lead to merging of mold features. Designs must include extra space between channels to account for this. (b) Bottom view of a PDMS device cast from an early mold. Due to adhesion of PDMS to the mold substrate and subsequent tearing during mold removal, nearly all crossed-channel valve membranes are missing (2 are circled in red). This problem was solved by ensuring very complete VSO solvent drying after support wax removal. (c) Comparison of an intact valve (left) and a torn membrane (right) viewed from the bottom. In the intact valve, the control channel, oriented top to bottom, crosses behind the fluid channel, oriented left to right. When the membrane is damaged, the channel interiors are physically connected. (d) Micrograph of PDMS fragments on the silicon wafer after melting of the wax mold. These fragments include the missing valve membranes in *c*. (e) Comparison of an intact valve (left) and one with a hole through the membrane. Such smooth-edged ruptures are believed to be caused by air bubbles not removed during degassing or perhaps by defects in the mold itself due to printing artifacts. (f) Micrograph of two valves, the right one having a small chunk of PDMS missing (circled in red), thus joining the fluid channel (running diagonally from bottom left to top right) to the adjacent control channel support post. This is a less severe form of the problem in *b* and is solved in the same manner. (g) Image of the silicon wafer after mold removal illustrating the presence of small PDMS fragments corresponding to the missing parts in *f*.

This section describes a number of the mold patterns that were designed to develop the molding protocol and ultimately to demonstrate pressure-actuated microvalves.

### 6.4.1 Test patterns

Noticing a discrepancy between our initial design files and the printed wax mold, we designed test patterns to explore three aspects of printer performance: (A) minimum lateral gap between features; (B) minimum lateral feature size (line width); and (C) minimum reliable vertical gap between features.

Pattern A (designed by George Maltezos) consisted of a series of small blocks separated from a wall by progressively smaller distances. Visual inspection of printed molds under a stereoscope revealed that separations of less than  $65\ \mu\text{m}$  in the *designed* mold resulted in merging of features in the printed wax.

Pattern B consisted of a series of short walls protruding perpendicularly from a long wall, separated from one another by gaps of  $400\ \mu\text{m}$  and gradually increasing in width from  $100\ \mu\text{m}$  up to  $300\ \mu\text{m}$ . In the vector mode of printing, designs are printed as outlines first; thus each of the short walls was printed in at least two passes (for the outer edges). For all feature widths of  $130\ \mu\text{m}$  and less, these passes completely overlap (by inspection of the ModelWorks file) and not surprisingly the printed features are roughly the same size. We observed a minimum printed line width of about  $200\ \mu\text{m}$  (up to  $300\ \mu\text{m}$  depending on ink-jet nozzle condition), with widths of larger features consistently in excess of the designed size by about  $70\ \mu\text{m}$ . This is roughly in agreement with the minimum gap test, as it suggests that each feature overflows its designed size by at least  $35\ \mu\text{m}$  on all sides. Based on the *worst case* overflow ( $85\ \mu\text{m}$  each side when print quality is poorest), we separated non-contacting features on later designs by at least  $200\ \mu\text{m}$  in the lateral direction to ensure separation in the actual mold. The test was performed with the pattern oriented in two different directions. We observed no significant difference in minimum width between the two cases; however, there was significantly less debris trapped between walls when they protruded in a direction

parallel to the movement of the milling head. In later designs, we thus aligned fluid channels with the milling direction where possible to reduce debris buildup that can lead to valve failures.

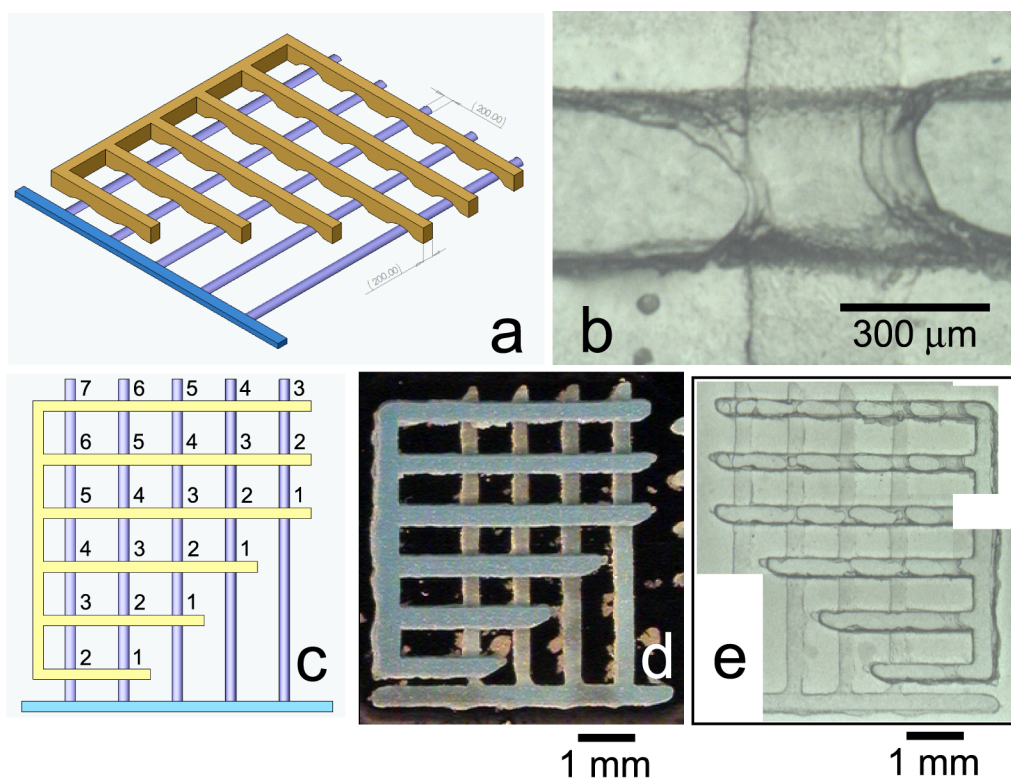


Figure 6.6: **Test of minimum vertical gap in wax molds.** (a) 3D design of test pattern used to determine the minimum vertical gap that could be used in wax molds. The bottom channels have a series of different heights, and the top channels have a series of different clearances through which the bottom channels pass; thus many different gap thicknesses are represented in the design. During casting, a gap between channel structures on the mold becomes a polymer membrane between two empty channels. (b) Photograph of an intact membrane in a PDMS device (bottom view). (c) Top view of the design indicating the thickness (in number of  $12.7 \mu\text{m}$  layers) of the gap between each pair of crossed channels. (d) Photograph (top view) of a printed mold after removal of the support wax. (e) Composite of three photographs of the PDMS device cast from the mold (bottom view). Note that membranes are broken or missing at gaps of 4 layers or less.

Based on the method of operation of the Solidscape printer, a 1-layer vertical gap between features in a design should in principle be faithfully reproduced in the printed mold. Pattern C is an array of push-down valves designed to test this (see Figure 6.6). It consists of 5 fluid channels in one direction crossed by 6 control channels in the perpendicular direction. The fluid channels have a circular arc profile and are printed directly on the substrate. Different channels have different heights, ranging from 3 to 7 layers, where each layer is  $12.7 \mu\text{m}$  thick. From the side, control channels appeared as a series of arches spanning the fluid channels, each control channel having arches of a different

height in the range of 5 to 10 layers. Vertical gaps between channels thus ranged in thickness from 1 to 7 layers. Due to the difficulty in visualizing the gap between channels in the mold and because we were interested in the minimum reliable gap thickness in actual microfluidic devices, we assessed the results of this test by inspection of a PDMS cast from the mold. Valve membranes less than 4 layers thick were missing or damaged in all cases. Some 4-layer membranes and all thicker membranes remained intact. These results suggested that subsequent designs should have at least 5 layers ( $64\ \mu\text{m}$ ) of clearance between crossing structures to ensure reliable separation in the cast device. This test was performed at a time when we were still having difficulty completely drying the VSO solvent after support wax removal; thus we suspected the reason for membrane breakage was damage during the wax removal stage due to small pieces of PDMS bonded to the mold substrate. However, later devices built with our optimized fabrication protocol were consistent with these results. The cause of the missing and broken membranes is not clear. It is possible that dust and debris is trapped between the channels during printing leading to a fragile, perforated membrane in the cast device, or perhaps the degassing process is not effective and tiny air bubbles remain trapped between the channels preventing PDMS prepolymer from flowing in to form the valve membrane when casting. The presence of trapped debris may help to stabilize such air bubbles. One additional possible cause is incomplete removal of support wax; however, this is unlikely since interchannel gaps viewed from the side under a stereoscope did not reveal any remaining support wax.

## 6.4.2 Microvalves

Two valve architectures were designed and tested to demonstrate the capability to implement active microfluidic devices with our molding process—a tube-like valve architecture and a crossed-channel architecture.

### 6.4.2.1 Tube valve architecture

George Maltezos designed and successfully actuated a PDMS valve with the architecture depicted in Figure 6.7. Fluid flows through a hollow PDMS tube (much like a short piece of silicone tubing)

surrounded by a chamber of air. The tube has a tall narrow hexagonal cross-section that is pinched shut when the surrounding air chamber is pressurized, thus closing the valve and blocking fluid flow. The length of the tube was typically 1–2 mm, and the designed thickness of the tube walls was typically  $100\ \mu\text{m}$ , resulting in less than  $50\ \mu\text{m}$  walls in the cast part.

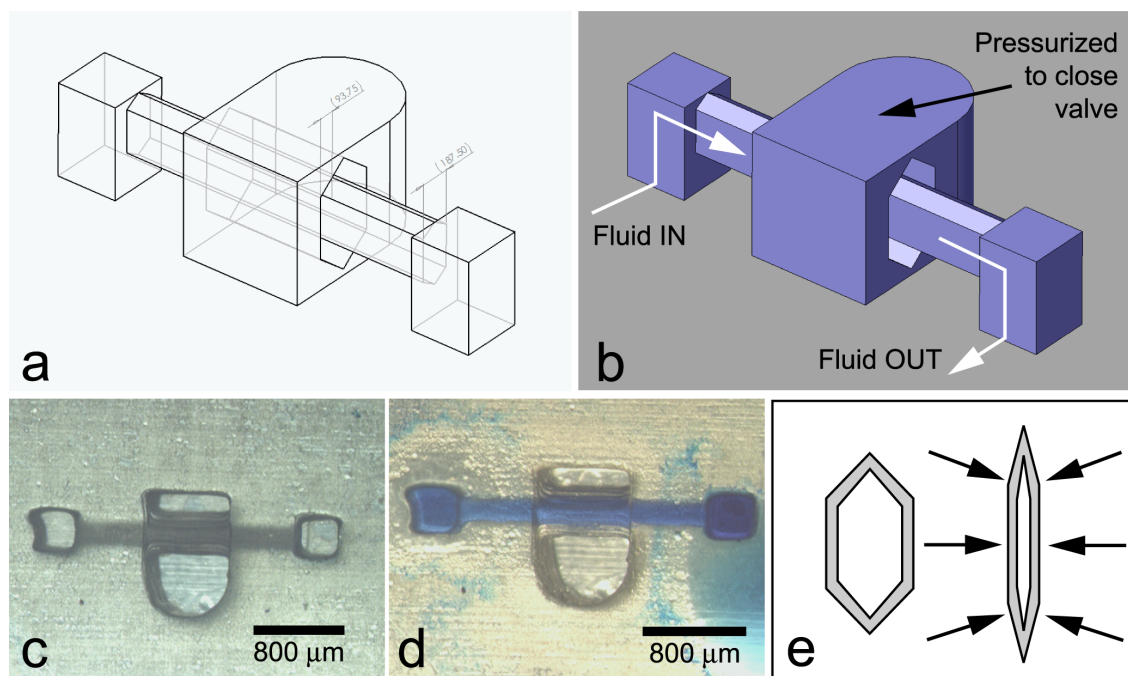


Figure 6.7: **3D tube valve.** (a,b) Design drawing (hidden line view and shaded view) for the mold for a 3D microfluidic tube valve. The central bar becomes the fluid channel in the cast device while the gap between this bar and the outer structure becomes the polymer wall of this channel. The outer structure becomes a hollow air chamber that is pressurized to close the valve. (c) Photograph of valve cast in PFPE. The roughness of the bottom surface is due to the use of a wax slab substrate for this particular mold. (d) Same valve with fluid channel filled with methanol (dyed blue with xylene cyanol FF). (e) Mechanism of valve operation. A cross-section of the tube inside the air chamber is shown. When the chamber is pressurized, the tube is squeezed shut to block the flow.

#### 6.4.2.2 Crossed-channel valve architecture

Having proved that devices with functional valves could be fabricated via 3D wax molding, we sought to demonstrate a crossed-channel valve to achieve a smaller valve footprint and to take advantage of the higher accuracy of the wax printer in the vertical direction to better control the thickness of the deflectable valve membrane. One additional difficulty with the tube valve design is the difficulty in curing *photopolymers* within the small gap that ultimately forms the tube wall. A crossed-channel

valve has less hidden material. For our tests, a push-down architecture was selected as, at the time, PFPE was not able to withstand the large deflections required in a push-up device.

An initial valve test pattern was designed by making several modifications to the layer thickness test described above. Fluid channel depths were all increased to 100  $\mu\text{m}$  (8 layers) to decrease the relative jaggedness of rounded profiles. If more typical PDMS channel depths (10–50  $\mu\text{m}$ ) were used, channel molds would be printed with just 1–4 layers, resulting in only a very crude approximation to a curved upper surface. Due to the uncertainty of the effects of jaggedness on valve performance, five different cross-sectional profiles were investigated in this design—one fluid channel was rectangular, three were trapezoidal, and one was bell-shaped. The latter has been shown theoretically to be the optimal shape in terms of minimal closing force [85]. Channel widths were increased to 300  $\mu\text{m}$  in the design (thus nearly 400  $\mu\text{m}$  in the actual device) to avoid the aspect ratio being too high. Control channels were supported on vertical posts such that when viewed from the side, they had a rectangular opening where they crossed fluid channels. Since we had been having problems with small pieces of PDMS being torn from the device at the edges of posts during mold removal, fluid channel spacing was increased and control channel posts were designed to be 400  $\mu\text{m}$  away from fluid channels. The six control channels crossed at different heights, such that vertical gaps (valve membrane thicknesses) ranged from 2 to 12 layers in 2-layer increments.

The printed mold and PDMS devices cast from the mold are shown in Figures 6.8 and 6.9. For redundancy, three copies of the pattern were printed on each mold—two at the designed size and one at twice this size. PDMS devices were cast on the molds and oxygen plasma bonded to cleaned glass slides. Numerous leaks prevented valves from being properly pressurized in all devices; however, we observed partial membrane deflection at 25 psi in one device. Despite this failure, several interesting observations could be made regarding the molds and PDMS devices. First, inspection of the devices confirmed the results of the thin-layer test, in that all valves with 2-layer membranes were broken, while some 4-layer membranes and all thicker membranes were intact. Curiously, on the double-sized mold, some of the valves with an 8-layer membrane had broken membranes. If failed membranes are caused by air bubbles, this result may suggest that degassing depends not only the gap thickness but

also the gap width. Second, examination of molds under a microscope revealed a peculiar artifact: the fluid channels were not uniform along their length. Rather, they undulated in width and height, becoming largest when passing under control channels and smaller in regions in between. There is no evidence of this in the ModelWorks file, so it is unclear how this effect arises. Perhaps it is related to the failure of valve membranes less than 4 layers thick. Third, the large number of fluid channels that were merged with control channel posts, due to missing chunks of PDMS, indicated that the lateral spacing of 400–800  $\mu\text{m}$  was not always sufficient to prevent such leaks. However, subsequent improvement in the wax removal procedure solved this problem, obviating the need for a change in design rules for the next design iteration. One final observation was the presence of thin PDMS flaps covering parts of fluid channels and control channel posts at the bottom surface of the cast device. These areas should be open since the wax features from which they are cast are in contact with the mold substrate. This artifact therefore indicates that the liquid PDMS prepolymer is sometimes able to flow underneath wax structures attached to the mold substrate. It is not known why this occurs—perhaps the wax-substrate adhesion is relatively poor, or surface tension forces dislodge features during immersion and removal of the mold from the VSO solvent, during evaporation of VSO, or during pouring or degassing of the PDMS prepolymer. For the most part, these flaps were not problematic since the bottom surface of the device was intended to be sealed anyway by bonding to a glass slide. However, they did occasionally interfere with bonding if they folded over the bottom surface, locally lifting the device from the substrate. The spurious flaps would also interfere if one wanted to perform *in situ* chemical synthesis on a derivatized glass surface, for example.

To deal with the problem of leaks and to facilitate valve testing, the design was again modified. Valve architecture was maintained, but the height and width of fluid channels was reduced to 65  $\mu\text{m}$  and 200  $\mu\text{m}$  (actual size), respectively. In addition, the layout was simplified to have only a single line of valves. The control channel was broken into short segments, isolating valves such that failure of one would not prevent all others from being pressurized. Multiple identical valves were included in case some failed. After observing many of the control channel segments fall off of the glass mold substrate during removal of support wax, the segments were enlarged to increase their surface

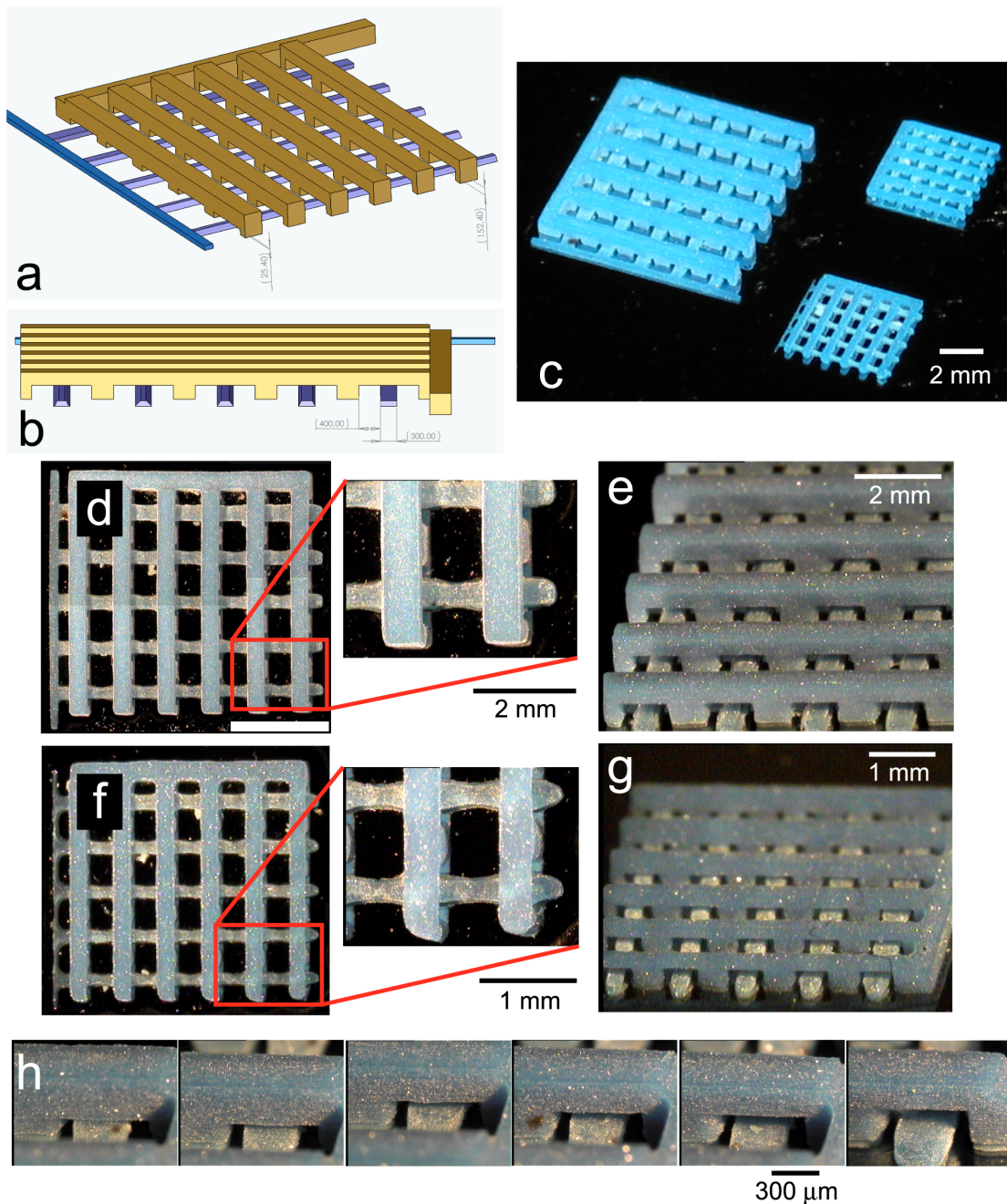


Figure 6.8: **Design and printed molds for crossed-channel valve tests.** (a) Design of the valve array test chip. Six control channels (gold) cross five fluid channels (blue). Control channel gaps become progressively larger, from 2 layers ( $25\ \mu\text{m}$ ) to 12 layers ( $152\ \mu\text{m}$ ). (b) End view of the design. All fluid channels are  $100\ \mu\text{m}$  tall but have different cross-sectional profiles. Note that all of the following photographs reflect molds printed with a very similar, but not identical, design—fluid channels are spaced more closely together. (c) Photograph of 3 molds printed on a silicon wafer. The largest was printed at twice the designed size. (d) Composite micrograph of the large mold (top view). Detail of a few channels is shown in the inset. (e) Tilted end view of the same mold, showing different channel profiles and the gradually decreasing gap thicknesses. (f) Photograph of one of the small molds (top view), scaled up for comparison with *d*, with detail shown in the inset. Since features on the small mold are close to the minimum feature size of the printer, printing artifacts are more prominent (debris and undulating fluid channel widths). (g) Tiled end view of the same mold. (h) Series of micrographs of the large mold illustrating gap sizes from 4 to 24 layers, in increments of 4 layers. (Same scale bar for all images.)

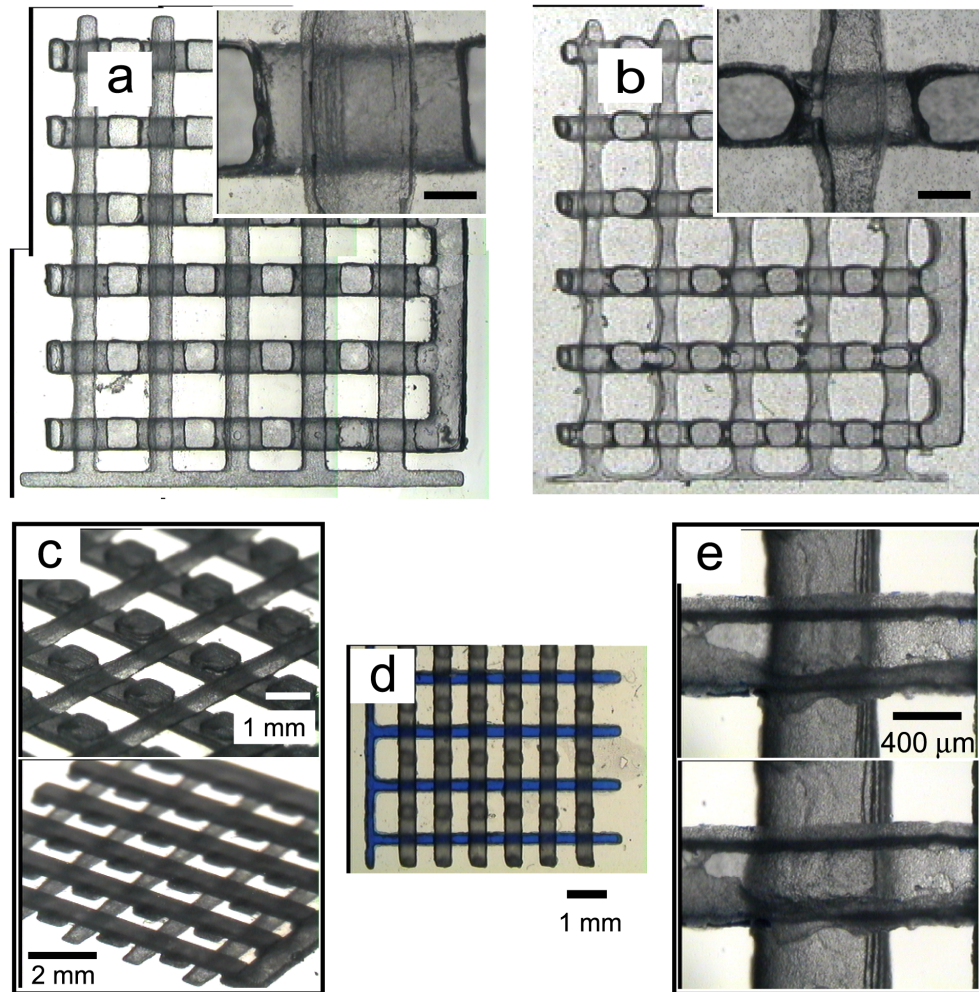


Figure 6.9: PDMS devices cast from 3D crossed-channel valve test mold. (a) Composite micrograph of PDMS device cast from large (double-sized) mold. Inset shows the detail of a valve viewed from below (bar:  $400\ \mu\text{m}$ ). The fluid channel is oriented top to bottom, while the control channel is oriented left to right. (b) Micrograph of PDMS device cast from normal-sized mold, at twice the magnification in *a*. Detail of a valve is shown in the inset (bar:  $400\ \mu\text{m}$ ). Note the pronounced non-uniformity in fluid channel width. (c) Tilted views of the large device from below (top) and above (bottom). (d) Micrograph of normal-sized device from above. Fluid channels are filled with water dyed blue with xylene cyanol FF. (e) Bottom view through the glass substrate of a single valve in the unpressurized (top, 0 psi) and pressurized (bottom, 25 psi) configurations. The fluid channel is oriented left to right, and the control channel is oriented top to bottom. When pressurized, the entire control channel expands, and at the crossing, the membrane bulges into the fluid channel, squeezing it towards the glass and partially blocking the flow.

contact and ended up looking like “H”s. (The fact that the segments fell off may be indicative of poor wax-substrate adhesion and could explain how the PDMS is able to leak beneath features.) This design, along with corresponding molds and devices, is illustrated in Figure 6.10.

To operate the valves, control channels (“H” structures) were filled with mineral oil and pressurized. If air was used, production of bubbles was observed in the fluid channel, resulting from diffusion across the valve membrane. Water (dyed blue with xylene cyanol FF) was introduced into the fluid channel at a fixed low pressure, typically 0–5 psi. Because the fluid is a better refractive index match to the PDMS than air, the surface roughness does not so severely obscure the valve, and its state can be observed visually. In one experiment, the valve was successfully closed at 27 psi, though there remained a significant leak flow rate, observed by watching the meniscus of the fluid move through the external tubing over a period of several hours. We could increase the fluid pressure to about 9–10 psi before the valve was forced open and the leak flow rate suddenly increased. In another experiment with a different PDMS device, we observed that 8 psi fluid pressure forced open a valve pressurized to 30 psi. Incomplete valve closure was presumably due to the approximately square profile of the fluid channel, which is difficult to close completely in any device, and due to the roughness (2–3  $\mu\text{m}$  bumps) of the top of the fluid channel due to the wax mold. The latter is the same effect that prevents the whole device from being sealed to a substrate, if the mold is printed on a wax slab support. The leak rate was quite slow at 30 psi control channel pressure. It may be possible to achieve more complete actuation simply by further increasing the pressure. Such *over-pressure* can also be achieved at the same external pressure by decreasing the valve membrane thickness. It may also be possible to improve valve sealing by decreasing the roughness of the channel features on molds. We attempted to achieve this by heating near the melting point; however, structures sagged and roughness was not decreased. Another attempt—prolonged exposure of molds to a solvent vapour (acetone)—resulted in significantly *increased* roughness. Lastly, we attempted to perform smoothing during mold fabrication by pressing a heated flat surface against the pattern after each milling step. Technically, this needs only to be done after the layer in which the uppermost part of the fluid channel is printed; however, smoothing all layers would improve

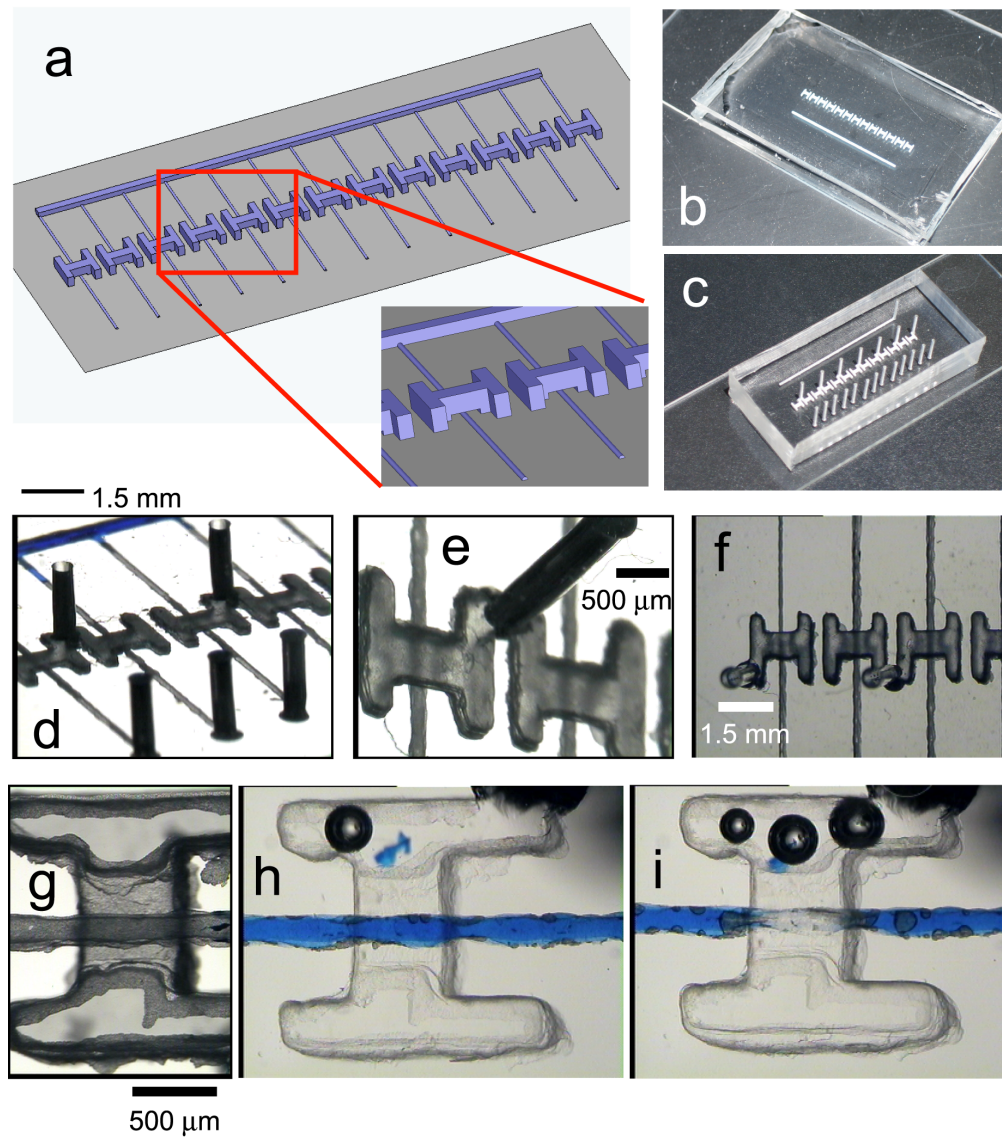


Figure 6.10: **Design and testing of “H” valve.** (a) Design drawing of the pattern of “H” valves. Each “H” is a short segment of a control channel crossing a fluid channel, as shown in the detailed inset. (b) Photograph of PDMS cast on a mold printed on a 2×3 inch glass microscope slide. (c) Photograph of same device after wax mold removal, hole punching, and plasma bonding to a 1×3 inch cleaned glass slide. (d) Micrograph of device showing several “H” valves and holes punched to access the channels. A closeup of two valves from above is shown in (e). In each, the path of the fluid channel is faintly visible under the center of the “H”. (f) Bottom view of several valves. The fluid channels are printed at the minimum feature width and therefore show considerable irregularity due to individual droplet effects. (g) Micrograph of a single valve, taken through the glass substrate. The fluid channel runs left to right and is sealed by the glass, as are the sides of the “H”. The central region is the valve—the control channel (oriented top to bottom) expands when pressurized and flattens the fluid channel against the glass to close the valve. The high surface roughness of the fluid channel surface is evident. (h) Single valve in the open configuration. The blue fluid is water dyed with xylene cyanol FF at 1 psi. The control channel (“H”) is filled with mineral oil. (Same scale as *g*.) (i) The same valve in the closed configuration with the mineral oil pressurized to 27 psi. Flow in the fluid channel is stopped. The circles are air bubbles in the mineral oil that disappeared about 30 minutes later.

visibility through the device. Unfortunately, using a silicon wafer and small weight heated to 60°C significantly damaged the support wax in the mold and had no effect on the build wax surface.

Additional modifications were also made to improve valve closure. We attempted printing shallower fluid channels (1–3 layers) but observed channels to be collapsed shut after plasma bonding. We have also fabricated devices with a quasi-rounded channel profile and with a push-up valve architecture. The push-up architecture not only gives potentially reduced actuation pressures, but the rough surface of the valve membrane should seal better to another PDMS surface than to glass [187]. However, only a marginal decrease in leak rate was observed in these push-up valve devices. An additional strategy is to first pattern the mold with rounded channels for the fluid channels by some other means (e.g., with photoresist) and then to print the suspended wax structures for the control channels on top of this. To attempt this will first require devising a means to align the printhead with the photoresist pattern.

The crossed-channel valve design is essentially the same as that used in multilayer PDMS microfluidic devices cast from photoresist molds. Once satisfactory valve fabrication and operation are achieved, this technology should therefore be suitable for any applications in which 2-layer architectures are already used. For example, Figure 6.11 shows a design for a 4×4 combinatorial array synthesizer (see Chapter 7) along with molds and devices that were fabricated. These particular devices were non-functional due to this early design not conforming to the design rules we later developed, but they give an approximate sense of the possible valve densities and device complexities.

### 6.4.3 Fully suspended structures

As described above, the polymer cast of a three-dimensional inverse channel network mold is not a finished microfluidic device—an adhesion step is still necessary to bond this polymer to a suitable flat substrate. This step seals the “floor” of all channel and support structures that are open at the bottom surface because the corresponding mold features were in direct contact with the mold substrate.

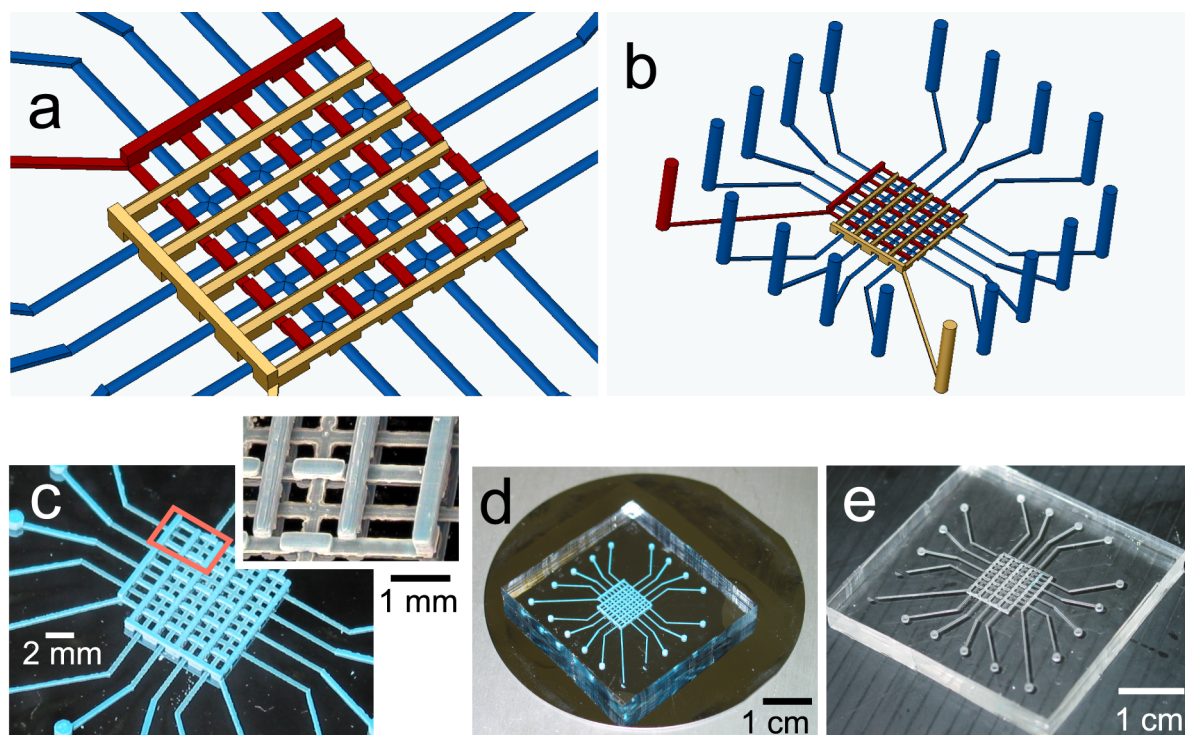


Figure 6.11: **Microfluidic device for 4×4 combinatorial array synthesis.** (a) 3D design for the central component of a microfluidic combinatorial array synthesizer (see Chapter 7). A grid of fluid channels (blue) is crossed by two sets (red and gold) of control channels in perpendicular directions. Actuating one set of control channels closes off all flow in one direction, forcing fluid flow through the device along 4 parallel fluid channels in the perpendicular direction. Carefully orchestrated delivery of reagents in fluid channels combined with alternation of flow direction allows for combinatorial synthesis of an array of compounds. (b) Overview of the entire design including posts that become inlet/outlet holes in the final device. Posts were later eliminated from the design due to their long mold fabrication time (many layers) and due to difficulties fabricating tall narrow structures. (c) Photograph (after support wax removal) of a wax mold with this design printed at double size on a silicon wafer. A detailed micrograph of the area inside the red box is shown in the inset. (d) Photograph of PDMS cured on the mold. (e) Photograph of PDMS device after melting and dissolving the wax mold.

In comparison with multilayer fabrication of PDMS microfluidic devices, we have demonstrated that three-dimensional molding eliminates the bonding step between device layers. In principle, it is also possible to eliminate the device to substrate bonding step as well. Microfluidic devices require inlet and outlet holes to connect to the outside world. On the mold, these could be represented by solid posts. With a sufficient number of carefully spaced posts, one could imagine fabricating the mold upside-down, supported entirely by these inlet and outlet posts. (Imagine an upside-down version of Figure 6.11b.) A thick polymer layer could be cast to completely encapsulate such a mold, thus forming a completely enclosed fluidic network after mold removal. The channel network must be carefully routed such that all beams (inverse channels) can be fully supported by posts without sagging. Sagging will result in altered channel shapes and, for crossed-channel valves, will affect the spacing between the fluid and actuation channels, resulting in unpredictable valve membrane thickness (and hence actuation pressure). Control channels pose a particularly difficult challenge since in multilayer PDMS devices these are typically implemented in a dead-end fashion with only one inlet and no outlet. Suspending an entire inverse control channel by a single post will be impossible in general; however, one could insert one or more extra posts into the design for mold fabrication and then plug these extraneous inlets in the final microfluidic device to allow the channels to be pressurized.

To reduce the possible adverse impacts of sagging, an alternative valve architecture could also be considered. A tall thin channel could possibly be actuated from one side [269], or a tube architecture could be used. In such designs, the critical dimension is in the lateral direction, and the vertical alignment is less critical.

I created several 3D designs to evaluate the ability of various channel cross-sections to avoid distortion when spanning long distances. However, the milling head of the Solidscape printer tends to topple tall thin posts and break long thin structures during printing if they are not attached to the mold substrate, and these patterns were never successfully fabricated. Since, by this time, bonding issues in solvent-resistant polymers had been resolved, efforts in this direction were suspended, and attention was focussed on development of working valves.

## 6.5 Discussion

### 6.5.1 Summary

In summary, we developed a method to fabricate microfluidic devices by replication molding in a single step from 3D wax molds using a commercial rapid prototyping machine. After numerous iterations of device designs and protocol modifications, we demonstrated devices having functional microvalves—both a tube architecture and the crossed-channel architecture commonly used in multi-layer PDMS devices—as a proof of principle. We also showed that other, solvent-resistant, polymers (PFPE and Sifel) are compatible with this technique.

Our 3D molding technique offers several significant advantages when compared with other fabrication methods. Fabrication is simplified as the mold itself is printed entirely automatically, and microfluidic device construction requires no alignment or layer-bonding steps. Elimination of layer bonding enables accelerated exploration of new elastomer materials, as valve performance can be evaluated to screen materials before undergoing the lengthy process of developing and optimizing a layer-bonding protocol. Compared with stereolithography, a much wider variety of device materials can be used since there is no requirement for photosensitivity or transparency. 3D molding also makes it very simple to implement topologically complex fluidic networks, many layers of valve control channels, or geometrically complex fluidic and optical structures.

There are a few drawbacks as well, perhaps the most serious at this time being the printing resolution. We found practical lower bounds of 200–250  $\mu\text{m}$  in channel width, 400  $\mu\text{m}$  in channel spacing, 4–5 layers (51–64  $\mu\text{m}$ ) in valve membrane thickness to avoid breaks and leaks, and about 3–4 layers (38–51  $\mu\text{m}$ ) in channel depth to avoid collapse due to the large width. There is probably some room for improvement of the ink-jet technology itself, perhaps by switching to other printing materials, as droplet sizes down to 20–30  $\mu\text{m}$  droplets have been demonstrated with other fluids, and sizes down to about 10  $\mu\text{m}$  are thought to be possible [34]. Pushing past 10  $\mu\text{m}$  has only been possible by lithographically patterning the substrate surface prior to printing, a process not suitable for three-dimensional objects since it only affects the first printed layer. To reduce the long printing time that

would be associated with such high-resolution printing, hybrid droplet schemes have been considered in which the outer edges are printed slowly with very tiny droplets while the internal regions are filled more quickly using much larger droplets. Resolution in the  $z$ -direction can presumably also be improved with the use of higher precision motors on the build platform. However, surface roughness and incomplete dust and debris removal will have to be addressed before additional resolution would be useful. An additional drawback is that sacrificial molds cannot be reused. Though printing and dewaxing a 3D mold of 1–2 mm height takes no longer than photolithographically patterning 2D molds for multilayer devices, the average microfluidic device fabrication time is much shorter for multilayer devices since a 2D mold can be reused many times. Average 3D mold fabrication time can be reduced by printing batches of multiple molds on the 6-inch build platform, as additional molds do not incur additional wax-cooling or milling time.

Many techniques exist for constructing three-dimensional microfluidic devices, each having particular capabilities and limitations, as reviewed in Section 6.2. As with any technology, one must weigh the benefits and drawbacks in the context of a particular application and choose accordingly among alternative fabrication methods.

### 6.5.2 The future of 3D fabrication

3D fabrication is inherently more complicated than 2D fabrication, and it is worthwhile to consider when the additional complexity is warranted. Indeed, for relatively simple assays and reactions, two dimensions are adequate, as several commercial products and the huge volume of literature illustrate. However, the third dimension can be exploited in a number of useful ways, sometimes enabling applications that would otherwise be impossible. I have already discussed the benefits of using 3D fabrication to eliminate layer-layer bonding steps in microfluidic devices. This section will elaborate on its other uses.

In Chapter 2, I discussed the many advantages of crossed-channel elastomeric valves over alternatives for fluid manipulation. These microvalves require 3D fabrication to implement an independent layer of control channels a small distance above or below the fluid channel network. The con-

trol channels provide the actuation mechanism of microvalves and the connections between these valves and ports that connect to off-chip pressure supplies. Sophisticated control of fluids has been demonstrated, incorporating components such as multiplexers to help reduce the number of off-chip connections required and improve scalability [268, 274]. Additional layers of control can provide additional flexibility and further reductions in number of connections to the outside world. For example, Thorsen *et al.* [268] demonstrated an individually addressable array, in which  $N \times M$  chambers could be selectively purged using only one fluid input, one fluid output, and  $\log(N) + \log(M)$  control inputs. This is clearly far more practical than having one control input per chamber or even one input for every row and column. To permit efficient addressing of a chamber by its row and column, two multiplexers were used: one acted on fluid channels to direct fluid from a single inlet to the selected row; the other acted on column control channels to select a single column of valves that would be opened. The more “processing” that can be performed on-chip, the fewer external control connections are required. Additional layers afforded by 3D fabrication could provide additional space for routing channels in dense networks or enable more complex control schemes (see Figure 6.12). Several interesting control schemes have also been reported that take advantage of three dimensions, including tangential channel microfluidic switches that can be dynamically reconfigured using air pressure [126].

The third dimension has also proven useful in expanding the topological flexibility of fluidic networks by allowing fluid channels to cross over one another. This flexibility has been used to perform combinatorial chemistry [148], to solve graph theory problems in computer science [41], and to pattern proteins and cells on surfaces in complex arrangements [40]. Microfluidic devices have been used extensively in cell culture studies (see [164] for a review), largely in the areas of evaluating drug effects and tissue engineering (growth and repair of tissues). Microfluidic devices have been used to create mimics of spatially organized biological tissues, such as *in vitro* mimics of blood vessel walls consisting of three layers of different cell types [264, 263]. Sophisticated 3D devices have also been used for establishing precisely controlled microenvironments (substrate topology and composition, type and position of neighbouring cells, etc.) to study cellular responses such as

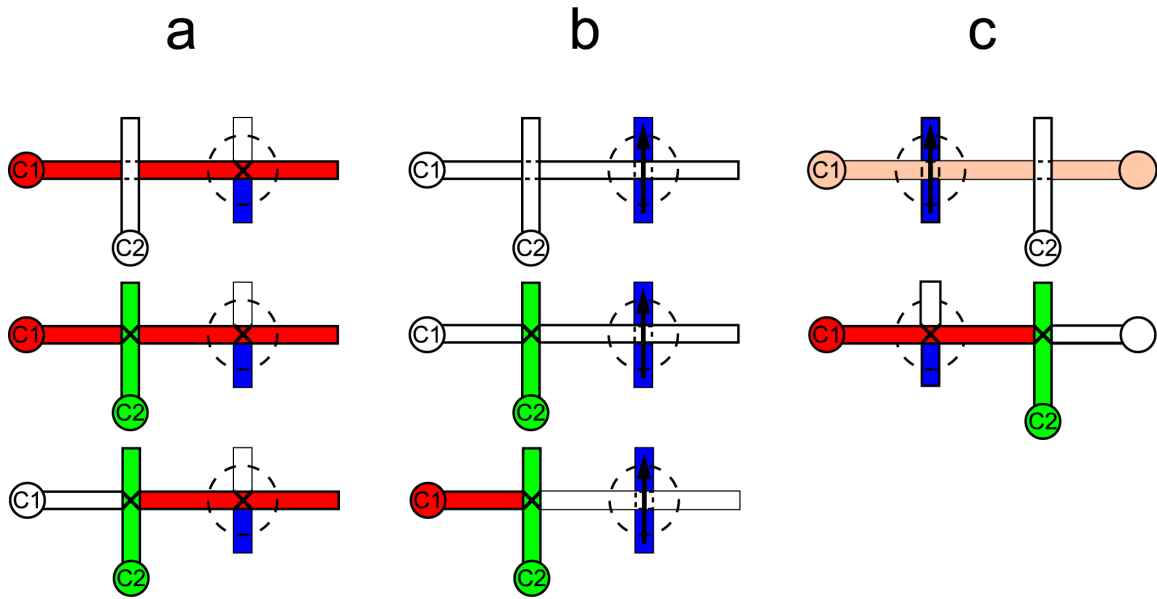


Figure 6.12: **Schematic of controlled control channel operation.** Additional channel layers enable new types of fluid control. For example, with three layers of channels, one can control not only the fluid channels, but also the control channels. Blue represents fluid channels in the bottom layer; red represents hydraulic control channels in the second layer; green represents hydraulic control channels in the third layer. So that the green channel can control the red one, it must use a higher pressure or some kind of force amplifier [2, 10]. Control channel inputs are designated by small circles. The valve controlling the fluid channel is encircled by a dotted line: an arrow along the fluid channel indicates it is open; an X indicates it is closed. (a,b) A state-preserving control. Actuation of control channel C2 locks the valve in the last state of control channel C1. In *a*, C1 is initially pressurized and the valve is closed (top). When C2 is pressurized, the pressurized fluid in the rightmost segment of channel C1 is trapped (middle), such that the valve remains closed even if C1 is later released (bottom). Similarly, *b* shows the operation if C1 is initially unpressurized (top). When C2 is pressurized (middle), it blocks C1. Even if C1 is subsequently activated, the pressurized fluid cannot reach the valve and the fluid channel remains open, thus preserving the initial state prior to C2 activation. (c) A boolean “AND” control. In this arrangement, the valve is closed only if both control inputs (C1 and C2) are pressurized. C1 contains an open outlet port at right so that it is impossible to build up pressure in the channel. Only by also activating C2 is the outlet blocked, allowing sufficient pressure to build up inside channel C1 and close the fluid channel valve. Although not shown, if C1 is not activated, the valve remains open regardless of the state of C2. It may also be possible to construct an *AND* valve simply by having two control channels stacked above one another.

migration and remodeling [151]. Microfluidic devices have also been used to create and study living neural networks with controlled 2D architectures [108], and there is no reason to believe such studies couldn't be extended to 3D networks.

Certain microfluidic processes and devices rely on 3D geometrical variations for their efficient operation. For example, rapid mixing in the diffusion-limited turbulence-free laminar flow regime requires some technique to rapidly fold and elongate the fluid to reduce the diffusion distance. Chaotic advection has been used in passive mixers consisting of serpentine channels with flow alternating between perpendicular planes [171] or channels with a staggered groove pattern in one of the channel walls [258]. (The latter can also perform additional novel functions such as controlling plug dispersion and positioning narrow streams within a channel [257].) In addition to these passive designs, active mixers have been demonstrated [35], including a rotary mixer utilizing three microvalves (in a second channel layer) as a peristaltic pump [43]. 3D fabrication also offers flexibility in the design of other components such as filters for removing particular contaminants [62], or traps for beads (to perform separations or solid phase synthesis) or for biological cells. In our lab, we have demonstrated active filters/traps consisting of partially closed valves, with the unique feature that the "pore" size can be adjusted or removed by controlling the valve pressure. 3D fabrication techniques have also proven useful to fabricate channels with unprecedented aspect ratios and long lengths for rapid mass or heat exchange [181].

In the area of integration of microfluidics with electronics and optics, 3D microfabrication technologies have been used to fabricate fluidic networks in place on top of silicon circuits, eliminating the need for alignment and bonding steps, potentially decreasing manufacturing time and cost [151]. Stereolithography and other techniques may even permit *in situ* fabrication of complex shapes such as external fluidic connectors (possibly macroscopic) or receptacles for aligning optical fibers. Mizukami *et al.* [197] report the integration of a stereolithographically fabricated serpentine acrylic channel network onto a photosensor array microchip for real-time imaging of separations. Similarly, Tse *et al.* [271] reported a technique for stereolithographically fabricating a plastic microfluidic flow cell directly on top of a silicon microelectronic chemical impedance sensor. 3D fabrication may

also benefit the emerging field of optofluidics, permitting construction of complex fluid-filled optical elements.

Finally, 3D fabrication may be exploited simply to increase chip densities as it enables vertical stacking of components and provides more space for routing interconnections. Expanding into the third dimension also provides additional space for large reactors, for example, without using up all the chip real estate.

For these, and undoubtedly many currently unimagined reasons, it is likely that 3D fabrication will play an increasing role in microfluidics as device complexity increases and as devices are applied to an ever-increasing range of applications.

## **Acknowledgment**

This molding approach was first developed by George Maltezos in Axel Scherer's group at Caltech. I thank him for sharing the results of his original work, for helping to improve the device fabrication protocol and microfluidic device designs to the point where devices could be properly sealed to flat substrates and crossed-channel valves could be demonstrated, and also for taking the time to print numerous 3D wax molds for my work. I also acknowledge the assistance of Jaime Perez, formerly of Solidscape, and other Solidscape engineers in modifying the printing process to accommodate our needs.